

Effect of Deuterium Substitution on the Surface Interactions in Binary Polymer Mixtures

ANDRZEJ BUDKOWSKI,¹ JAKUB RYSZ,¹ FRANK SCHEFFOLD,² JACOB KLEIN,² LEWIS J. FETTERS³

¹ Institute of Physics, Jagellonian University, Reymonta 4, 30-059 Kraków, Poland

² Department of Materials and Interfaces, Weizmann Institute of Science, Rehovot 76100, Israel

³ Exxon Research and Engineering Company, Annandale, New Jersey 08801

Received 30 October 1997; revised 1 April 1998; accepted 18 May 1998

ABSTRACT: We have examined the effect of deuterium labeling on surface interactions in mixtures of random olefinic copolymers $[C_4H_8]_{1-x}[C_2H_3(C_2H_5)]_x$. Based on surface segregation data we have determined a surface energy difference χ_s between pure blend constituents. In each binary mixture components have different fractions x_1 , x_2 of the group $C_2H_3(C_2H_5)$, and one component is labeled by deuterium (dx) while the other is hydrogenous (hx). The mixtures are grouped in four pairs of structurally identical blends with swapped labeled constituent (dx_1/hx_2 , hx_1/dx_2). For each pair the surface energy parameter χ_s increases when the component with higher fraction x is deuterated, i.e., $\chi_s(dx_1/hx_2) > \chi_s(hx_1/dx_2)$ for $x_1 > x_2$. A similar pattern has been found previously for the bulk interaction parameter χ . This is explained by the solubility parameter formalism aided by the lattice theory relating the surface excess to missing-neighbor effect. χ_s has also an additional contribution, insensitive to deuterium swapping effect, and related to entropically driven surface enrichment in a more stiff blend component with a lower fraction x . Both enthalpic and entropic contributions to χ_s seem to depend on the extent of chemical mismatch between blend components. © 1998 John Wiley & Sons, Inc. *J Polym Sci B: Polym Phys* 36: 2691–2702, 1998

Keywords: surface segregation; polyolefin copolymers; deuterium labeling effect

INTRODUCTION

The bulk and surface thermodynamical properties of polymer mixtures have been a topic of considerable interest from a fundamental¹ as well as from an applications² point of view. Over the last decade much experimental and theoretical work has focused on model systems of polymer mixtures formed by molecules with different isotopic or/and microstructural composition.

Partial miscibility^{3,4} observed in isotopic mixtures has been attributed to cohesive energy dif-

ferences between the blend components. The same effect leads to the phase separation⁵ of isomeric blends composed of random olefinic copolymers. These copolymers, of mean composition $E_{1-x}EE_x$, where E and EE are linear diethylene—(C_4H_8)—and branched ethyl ethylene—($[C_2H_3(C_2H_5)]$)—groups, are molecules whose mean microstructure varies continuously with x from polyethylene ($x = 0$) to poly(ethyl ethylene) ($x = 1$). Cohesive energy differences due to isotopic and microstructural disparity could be coupled in the bulk interaction parameter χ : A considerable change in χ is observed^{6–9} in the mixtures of random olefinic copolymers caused by the swap of the component labeled by deuterium (label swapping effect).

Correspondence to: A. Budkowski

Journal of Polymer Science: Part B: Polymer Physics, Vol. 36, 2691–2702 (1998)
© 1998 John Wiley & Sons, Inc. CCC 0887-6266/98/152691-12

The enrichment by one of the components at the free surface observed in most isotopic mixtures¹⁰ has been explained by extending¹¹ the enthalpic arguments describing bulk interactions. These arguments predict a surface excess in the component with lower cohesive energy. Such predictions turn out to be wrong when additional entropy-related forces are present, for instance, driving the segregation of protonated but much shorter chains in isotopic mixtures.¹² A competition of enthalpic and entropic considerations is commonly advocated for real polymer blends.^{12–16}

Various entropy-based mechanisms have been proposed for different types of molecular architectures. The restriction of configurations available to linear chains is considered to play a decisive role when the components have different lengths^{12,17,18} or surface interactions.¹⁹ Long-branched chain additives are expected^{16,17,20} and observed^{17,21} to segregate preferentially at surfaces of linear polymer matrix because they act²⁰ as a collection of unconnected short linear chains. Short-branched polymers represented by random olefinic copolymers $E_{1-x}EE_x$ are modeled^{13b,15,22} as effective linear chains with tuned bond flexibility, or chain stiffness. Their blends form systems with stiffness disparity, similarly to the moieties of poly(ethylene propylene)–poly(ethyl ethylene) diblock copolymers.²³ Although preferential segregation of more flexible units is attributed^{15,22} to configurational entropy effects, a pronounced surface excess of the stiffer component is expected^{13,24,25} due to^{13b} packing entropy and entropy effects due to local rearrangements of segments at the surface. It was shown²⁵ that an entropic mechanism preferring more rigid segments might be of equal importance to one of purely enthalpic origin.

In a series of studies we examined the free-surface behavior of mixtures with stiffness disparity, composed of short-branched olefinic copolymers $E_{1-x}EE_x$: initial direct observations²⁶ of the complete wetting by the more flexible component (with higher EE content x) were followed by detailed studies^{26–29} monitoring surface segregation as a function of concentration, temperature, and blend components. An earlier discussion of some of these results²⁷ suggested that the driving potential for the surface enrichment is predominantly enthalpic, rather than entropic in origin.

This article focuses on the deuterium labeling effect observed for surface interactions. It allows us to separate the enthalpic and entropic

contributions, argued to be either strongly^{6–8} or weakly^{15b} sensitive to the change of the isotopic composition of the molecule, respectively. Cumulative analysis performed on the segregation data^{27–29} yields a better insight on the role and relative amplitudes of both enthalpic and entropic forces driving the segregation of copolymers with higher and lower EE fraction x , due to lower cohesive energy and due to higher stiffness, respectively.

This article is organized as follows. In the Results section we show the label-swapping effect as observed in segregation profiles and surface excess data. We briefly describe a mean field approach used to determine the concentration dependence of the compositional derivative of “bare” surface-free energy. In the Surface Energy Parameter section this is used to calculate the surface energy differences between blend components, represented for a given temperature by a dimensionless surface energy parameter χ_s . The main result of this section is the comparison of absolute magnitudes and of changes due to the label swapping effect between surface energy difference χ_s and bulk interaction χ parameters. The enthalpic contribution to χ_s is calculated in the Missing Neighbor Effect section, based on available cohesive energy density data. Its comparison with overall values of the surface parameter χ_s estimates its entropic part. It is found that the strength of both contributions seems to depend on the extent of chemical mismatch between blend components.

RESULTS

We have studied the effect of deuterium labeling on surface interactions in the blends of random olefinic copolymers $E_{1-x}EE_x$, whose molecular characteristics are given in Table I. In each binary mixture components have different fractions (expressed as percentages) x_1, x_2 of the EE group, and one component is labeled by deuterium (dx) while the other is hydrogenous (hx). The composition–depth profiles of the deuterated³⁰ or hydrogenated²⁷ component within the samples (normal to the free surface) were determined using nuclear reaction analysis.³⁰ The change of surface enrichment upon the exchange of the blend component labeled by deuterium is observed for pairs x_1/x_2 of isostructural mixtures ($dx_1/hx_2, hx_1/dx_2$). This label-swapping effect is illustrated by Figure 1(a) and (b) for the blend pairs 66/52 and

Table I. Molecular Characteristics of the $E_{1-x}EE_x$ Copolymers

Polymer dx/hx	N	a [nm]	f_D
$d38/h38$	1830	0.76	0.37
$d52/h52$	1510	0.72	0.34
$d66/h66$	2030	0.68	0.40
$d75/h75$	1625	0.64	0.40
$d86/h86$	1520	0.60	0.40

x is the % EE (ethyl ethylene) segment randomly distributed along each polymer backbone. N is the weighted-averaged degree of polymerization (polydispersity < 1.08 in all cases), f_D is the fraction of hydrogen replaced by deuterium on the dx chains, and a is the statistical segment length.

86/75, respectively. Figure 1(a) compares composition-depth profiles^{28,29} of the copolymer $x = 66\%$, obtained for mixtures $d66/h52$ (open symbols and dashed lines) and $h66/d52$ (solid symbols and solid lines) annealed at similar temperatures. Analogous profiles²⁹ of the blend component $x = 86\%$ are presented in Figure 1(b) for the blend pair 86/75. As the nuclear reaction analysis³⁰ profiling technique has limited depth resolution, the essential observable is the area under the surface peak [shaded in Fig. 1(a)] defined as surface excess Γ in the component with higher EE fraction x_1 ($x_1 > x_2$):

$$\Gamma = \int_0^{z(\phi_\infty)} [\phi(z) - \phi_\infty] dz \quad (1)$$

Here $z(\phi_\infty)$ is the distance from the surface ($z = 0$) to the plateau (ϕ_∞) in volume fraction $\phi(z)$ of the blend component A with EE content x_1 ($x_1 > x_2$).

We may deduce from Figure 1(a) that the excess Γ of the copolymer $x = 66\%$ at the surface is larger when this copolymer is deuterated. The opposite situation, when $x = 66\%$ is fully hydrogenous, results in a smaller excess. This pattern is in line with that observed previously⁹ for the bulk phase diagrams recalled in the inset to Figure 1(a) (for each blend we use the same notation in figure as in its inset). The critical point T_c , and hence, also the bulk interaction parameter χ , is higher for the $d66/h52$ blend than for the $h66/d52$ mixture (dashed and solid curve in the inset, respectively). A similar trend can be concluded from Figure 1(b) for the blend pair 86/75, i.e., for mixtures $d86/h75$ and $h86/d75$. Here also, the

surface and bulk interactions are both increased when the blend component with higher EE content ($x = 86\%$) is deuterated.

The main output of our segregation studies^{27–29} is the surface excess Γ evaluated at various temperatures as a function of bulk composition ϕ_∞ . The resolution in determining Γ was equal to ca. 10% of its absolute value for segregated deuterated copolymers, and it was additionally worsened by ca. 1 nm for the surface enriched by protonated chains. The analysis presented in this work is based on the segregation isotherms $\Gamma(\phi_\infty)$ determined for four isostructural blend pairs x_1/x_2 : 86/75, 75/66, 66/52, and 52/38 at temperatures ranging from 40 to 165°C. These results are illustrated in Figure 2 by a limited data set corresponding to annealing temperatures close to $T_{ref} = 100^\circ\text{C}$. It is supplemented by surface excess values $\Gamma(\phi_\infty)$ measured also for other temperatures whenever the temperature dependence²⁸ of $\Gamma(\phi_\infty)$ is not very strong. Open and solid symbols in Figure 2 correspond to mixtures with a deuter-

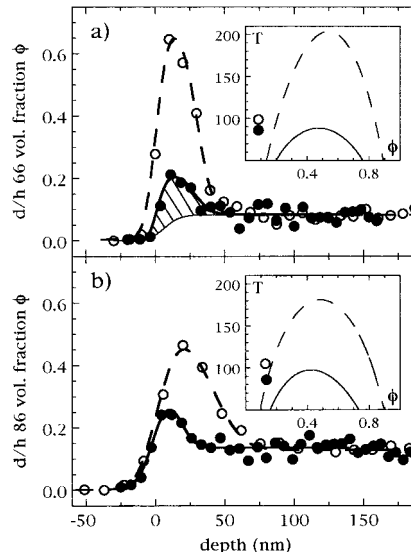


Figure 1. Isotope label-swapping effect as observed in blend pairs x_1/x_2 : 66/52 (a) and 86/75 (b). Composition-depth profiles^{28,29} of the copolymer x_1 ($x_1 > x_2$) across films of dx_1/hx_2 and hx_1/dx_2 annealed to equilibrium. The bulk compositions ϕ_∞ of the presented profiles are marked on corresponding phase diagrams presented in the insets. Open circles and dashed lines correspond to the dx_1/hx_2 blend, while solid circles and solid lines are for the hx_1/dx_2 mixture. Clearly the surface excess Γ (marked as hatched area for $h66/d52$ in (a)) increases when hx_1/dx_2 mixture is exchanged for the dx_1/hx_2 blend in line with the shift noticed⁹ for phase diagrams in the insets.

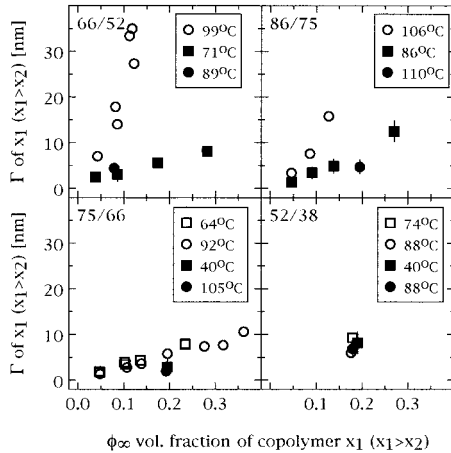


Figure 2. Representative surface excess $\Gamma(\phi_\infty)$ data of blend pairs $x_1/x_2 (x_1 > x_2)$: 66/52, 86/75, 75/66 and 52/38. Open and solid symbols correspond to the blends dx_1/hx_2 and hx_1/dx_2 , respectively. The resolution in determining Γ is marked by error bars, otherwise it is smaller than the size of symbols used.

ated blend component with higher (x_1) and lower (x_2) EE content ($x_1 > x_2$), respectively. We note that the amplitude of the change in surface excess Γ due to the label-swapping effect decreases from the 66/52, through 86/75 and 75/66 to the 52/38 blend pair. The same sequence of blend pairs is associated with a monotonic decrease of the difference in critical temperature $T_c(dx_1/hx_2) - T_c(hx_1/dx_2)$ (yielding values 116, 84, 68, and 27 deg, respectively⁹). This apparent relation between surface and bulk amplitudes of the label swapping effect is analyzed more precisely below. Because the surface excess Γ is a function of both bulk concentration ϕ_∞ and temperature, the quantitative analysis must be based on a model that includes these two dependences.

We start with briefly outlining the mean field (MF) theory,^{31–34} used to analyze our segregation data.^{27–29} The excess free energy F of the polymer mixture bounded by the surface is represented as a sum ($F = F_b + f_s$) of the bulk F_b and (“bare”) surface f_s free energies, dependent on the concentration profile $\phi(z)$ and its surface value ϕ_s , respectively. While the bulk free energy F_b is quite well understood, only simplified descriptions of f_s are available.¹¹ The F_b term contains a contribution due to concentration gradient plus the free energy of homogenous mixture $F_{FH} = [\phi/N_A]\ln \phi + [(1 - \phi)/N_B]\ln(1 - \phi) + \chi \phi(1 - \phi)$. Here, N_A and N_B are the polymerization indices of both blend components, and bulk interaction parameter⁹ χ depends on temperature. It is assumed that

the “real” composition profile $\phi(z)$ and its surface value ϕ_s are those that minimize the excess free energy F expressed within a MF approach. Then the formula for the surface excess $\Gamma(\phi_\infty)$:

$$\Gamma(\phi_\infty) = \pm \frac{1}{6} \int_{\phi_\infty}^{\phi_s} \frac{\sqrt{(1 - \phi)a_A^2 + \phi a_B^2}(\phi - \phi_\infty) d\phi}{\sqrt{\phi(1 - \phi)[F_{FH}(\phi) - F_{FH}(\phi_\infty) - \Delta\mu(\phi - \phi_\infty)]}} \quad (2)$$

allows us to determine the corresponding surface composition ϕ_s . The positive and negative sign in eq. (2) corresponds to the surface enriched^{27–29,31–33} (i.e., $\phi_s > \phi_\infty$) and depleted^{29,11b,34,35} (i.e., $\phi_s < \phi_\infty$) in copolymer x_1 , respectively. $\Delta\mu$ is the chemical potential difference between blend components, while a_A and a_B denote their statistical segment lengths. Using the values of ϕ_s obtained with eq. (2), it is possible to calculate the derivative of the surface-free energy ($-df_s/d\phi_s$), representing the driving force for segregation:

$$-\frac{df_s}{d\phi_s} = \pm \frac{\sqrt{(1 - \phi_s)a_A^2 + \phi_s a_B^2}}{3} \times \frac{\sqrt{F_{FH}(\phi_s) - F_{FH}(\phi_\infty) - \Delta\mu(\phi_s - \phi_\infty)}}{\phi_s(1 - \phi_s)} \quad (3)$$

The signs above are governed by the same convention as for eq. (2).

The procedure outlined in eqs. (2) and (3) yields for each singular segregation isotherm point $\Gamma(\phi_\infty)$ a corresponding locus of the “bare” surface-free energy derivative ($-df_s/d\phi_s$) plotted as function of concentration ϕ_s on so-called Cahn construction. This is illustrated in Figure 3 by the loci corresponding to the segregation data of the 86/75 blend pair plotted in Figure 2. The same types of symbols are used in both figures to relate different data sets: open circles correspond to $d86/h75$ at $T = 106^\circ\text{C}$, while black squares and circles to $h86/d75$ at $T = 86$ and 110°C , respectively. For each set an additional locus is calculated^{27–29} for lowest ϕ_s , based on interpolation between zero and the lowest measured $\Gamma(\phi_\infty)$ value. Marked error bars illustrate uncertainties due to limited resolution in determining surface excess Γ . The derivative ($-df_s/d\phi_s$) relation of the $h86/d75$ blend zeroes at surface concentration Q

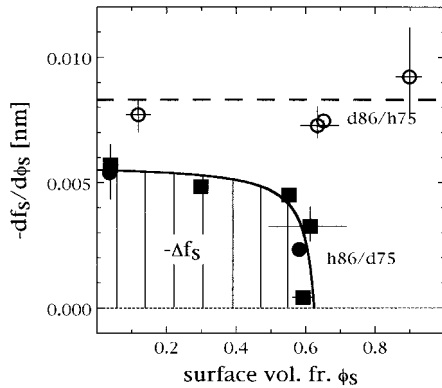


Figure 3. Cahn construction for the surface enrichment $\Gamma(\phi_\infty)$ data set presented in Fig. 2 for the blend pair 86/75. Loci describing the concentration ϕ_s dependence of the ‘bare’ surface free energy derivative ($-df_s/d\phi_s$) are determined for the d86/h75 blend at 106°C (open circles) as well as for the h86/d75 mixture (solid symbols) at 86 (solid squares) and 110°C (solid circles). Error bars illustrate uncertainties due to limited resolution in determining surface excess Γ . Lines denote best fits.^{27–29} The surface energy difference ($-\Delta f_s$) between components of the h86/d75 blend at 86°C is marked by dashed area.

< 1 . Negative values of ($-df_s/d\phi_s$) for surface concentrations $\phi_s > Q$ are excluded, as no surface enrichment in the d75 component was observed²⁷ for this mixture at similar temperatures. Limited resolution (of ca. 0.25 nm) in determining a related zero surface excess Γ results in an estimated uncertainty range ($-1 \cdot 10^{-3}, 0$) nm imposed on the ($-df_s/d\phi_s$) value for $\phi_s > Q$.

The question of curvature in the ($-df_s/d\phi_s$) vs. ϕ_s relation has been examined in our previous work.²⁷ Its origin was related³⁶ to composition gradient terms present in ‘bare’ surface energy f_s , reexpressed as a nonlinear function dependent only on ϕ_s . Elsewhere²⁸ we have observed a monotonic change of this curvature with temperature. For instance, the ($-df_s/d\phi_s$) loci corresponding to the d86/h75 blend at temperature of 178°C are similar to these plotted in Figure 3 for the h86/d75 mixture. Existing mean field theories^{11,35} allow for temperature variation of the relation ($-df_s/d\phi_s$) vs. ϕ_s . They also expect enrichment-depletion duality^{11b,34,35} and a critical wetting transition³³ to occur possibly for ($-df_s/d\phi_s$) going to zero at surface concentration $Q < 1$. The former effect has been recently observed²⁹ in our laboratory. Cahn constructions analogous to that presented in Figure 3 have been performed for other segregation data sets^{27–29}

and they constitute now the basis of further analysis.

SURFACE ENERGY PARAMETER

The concentration dependence is eliminated from our considerations when the force driving the segregation is described not by the derivative of the surface-free energy ($-df_s/d\phi_s$), but rather by its integrated form:^{27–29}

$$\Delta f_s \equiv f_s(\phi_s = 1) - f_s(\phi_s = 0)$$

$$= - \int_0^1 \left(-\frac{df_s}{d\phi_s} \right) d\phi_s \quad (4)$$

expressing the surface energy difference Δf_s between two pure blend components. The amplitude of Δf_s is, hence, obtained by integrating (see hatched area in Fig. 3) the relation ($-df_s/d\phi_s$) vs. ϕ_s . In all cases where the surface energy derivative goes to zero at concentration $Q < 1$, we assume its zero value also for surface concentrations $\phi_s > Q$, save that experiment reveals enrichment-depletion duality.²⁹ Related uncertainties estimated for zero ($-df_s/d\phi_s$) values contribute to the error bars imposed on the surface energy difference Δf_s . However the uncertainty in Δf_s is caused mainly by the scatter in the loci on the Cahn plot, originating from that in segregation data.

The procedure^{10a,37} expressed by eq. (4) has been shown to yield reasonable estimations of Δf_s (compare, e.g., refs. 10c and 38), although it assumes³⁹ a MF-type shape of the segregation profile $\phi(z)$. A more general approach^{10c} using the Gibbs adsorption equation (GAE) is plausible when not only the surface excess Γ but also surface concentration ϕ_s data are available: The GAE produces Δf_s values slightly higher (by ca. 20%) than those yielded by MF. Another origin of possible uncertainty in the calculated Δf_s is related to the precise value of bulk interaction parameter χ or alternatively to the location of phase diagram (compare, e.g., refs. 36 and 40). This factor can be neglected in our analysis because we always use binodals determined directly for identical blend films.⁹

The surface energy difference Δf_s may be expressed in terms of the difference $\Delta\gamma$ in a surface tension between blend components. Alternatively, it could be formulated in terms of the di-

dimensionless surface energy difference parameter χ_s defined per lattice site:

$$\Delta\gamma = \frac{k_B T}{V(T)} \Delta f_s \quad (5a)$$

$$\chi_s = \frac{\Delta f_s}{V^{1/3}(T)} \quad (5b)$$

The value of the segmental volume V , appropriate for different temperatures T and EE fractions x , is obtained from an empirical expression $V(x, T) [\text{\AA}^3] = (108.79 - 1.149 \cdot 10^{-2} x [\%]) + 8.1 \cdot 10^{-2} (T[\text{^\circ C}] - 23)$, fitting a wide range of corresponding experimental data.⁴¹

The existing MF theories only qualitatively account^{11,35} for the temperature variation of the surface tension difference between blend components. On the other hand, it has been established that the surface tension of simple liquids and polymers varies with temperature following the empirical Guggenheim formula:

$$\gamma(T) = \gamma_0 (1 - T/T_{cr})^{11/9} \quad (6)$$

where T_{cr} is an imaginary critical temperature of the polymer.^{42a} Parameters $\gamma_0 = 53.7 \text{ mJ/m}^2$ and $T_{cr} = 1030 \text{ K}$, were determined earlier^{42b} for the linear polyethylene ($x = 0$).

In Figure 4 we present the temperature variation of the relative difference in the surface tension $-\Delta\gamma/\gamma(T)$ between components of six isostructural blend pairs 66/52, 86/75, and 75/66 (the data of the 52/38 pair are not included here for the sake of clarity of presentation). Identical patterns mark symbols describing the same blend pairs x_1/x_2 ($x_1 > x_2$), while circles and squares are for dx_1/hx_2 and hx_1/dx_2 mixtures, respectively. The differences in surface tension $\Delta\gamma$ are calculated within MF based on segregation isotherms^{28,29} (larger symbols) and singular surface excess data^{27,29} (smaller symbols). For $\gamma(T)$, we take the relation for polyethylene ($x = 0$), because no data on $\gamma(T)$ for each copolymer $E_{1-x}EE_x$ are available. In all cases, the value $-\Delta\gamma/\gamma(T)$ does not exceed some 2%. The cumulative plot of Figure 4 suggests that the surface tension difference $-\Delta\gamma$ is monotonically decreasing with temperature. The rate of this reduction in $-\Delta\gamma$ seems to be described well by the formula [eq. (6)] in the wide temperature range between 40 and 150°C.

Our further analysis is based on the relative surface tension difference $-\Delta\gamma/\gamma(T)$ between

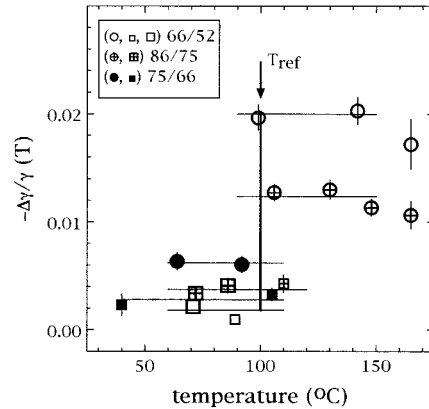


Figure 4. The relative surface tension difference $-\Delta\gamma/\gamma(T)$ between components of 6 mixtures, grouped in 3 blend pairs x_1/x_2 ($x_1 > x_2$): 66/52, 86/75 and 75/66, presented as a function of temperature. Differences $\Delta\gamma$ are related to $(-\Delta f_s)$ values determined for segregation isotherms (larger symbols) and singular surface excess data (smaller symbols), while $\gamma(T)$ is given by eq. (6). Circles and squares correspond to blends dx_1/hx_2 and hx_1/dx_2 , respectively. Error bars are due to uncertainties in $(-\Delta f_s)$. Solid lines denote average $-\Delta\gamma/\gamma(T)$ values around $T_{ref} = 100^\circ\text{C}$.

blend components, evaluated at a reference temperature $T_{ref} = 100^\circ\text{C}$. Determined $-\Delta\gamma/\gamma(T)$ values (see Fig. 4) are always higher for the mixtures with a deuterated blend component with higher (circles) than with lower (squares) EE content. This pattern is almost undetectable for the 52/38 blend pair with the $-\Delta\gamma/\gamma(T)$ values at T_{ref} equal to 0.92(13)% and 0.87(17)% for $d52/h38$ and $h52/d38$, respectively. Again, the magnitude of the isotope label-swapping effect, expressed now more precisely by the change in $-\Delta\gamma/\gamma(T_{ref})$, is highest for the 52/66 blend pair (open symbols in Fig. 4) and decreases through 86/75 (symbols with crosses) and 75/66 (solid symbols) to the 52/38 blend pair.

Now we determine the relation between surface χ_s and bulk χ parameters at a reference temperature $T_{ref} = 100^\circ\text{C}$. The values of surface energy difference parameter χ_s are determined based on evaluated $-\Delta\gamma/\gamma(T_{ref})$ data (Fig. 4). Uncertainties in χ_s are due to the dispersion in $-\Delta\gamma/\gamma$ around the plateau values. To calculate relevant values of bulk interaction parameter χ we eliminate first its concentration dependence. Here and in the next section we approximate its complete formula $\chi(T, \phi) = (A'/T + B)(1 + v\phi)$ by a simpler Flory–Huggins form $\chi = A/T$. For the polymers studied here this last formula

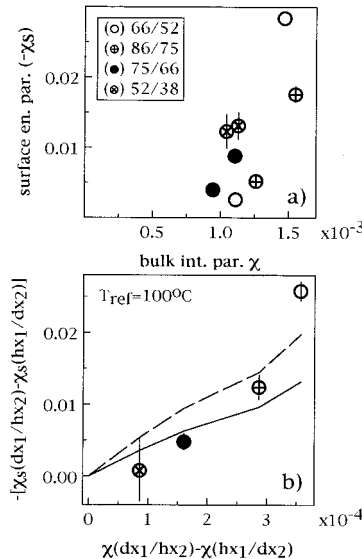


Figure 5. (a) The surface energy difference parameter χ_s plotted as a function of bulk interaction parameter χ for blend pairs x_1/x_2 ($x_1 > x_2$): 66/52 (○), 86/75 (⊕), 75/66 (●) and 52/38 (⊗) at a reference temperature ($T_{ref} = 100^\circ\text{C}$). For each pair the point with higher ($-\chi_s$) and χ values corresponds to the dx_1/hx_2 mixture. (b) The corresponding change in surface $-\left[\chi_s(dx_1/hx_2) - \chi_s(hx_1/dx_2)\right]$ and bulk $\left[\chi(dx_1/hx_2) - \chi(hx_1/dx_2)\right]$ parameter due to the isotope label swapping effect. Data for different blend pairs are marked as in Fig. (a). The solid and dashed lines mark predictions yielded by the r.h.s. of eq. (12) for $z_s/(z - 2)$ equal to 0.5 and 0.75, respectively.

was shown to describe well⁹ the temperature relation whenever the ϕ dependence is not relevant. We use χ values evaluated⁹ at T_{ref} for the Flory-Huggins form.

Figure 5(a) presents the relation between the surface energy difference χ_s and the bulk interaction χ parameters determined for the eight mixtures of four isostructural blend pairs x_1/x_2 ($x_1 > x_2$) with exchanged-labeled component. Figure 5(b) compares the magnitude of the label-swapping effect observed for surface and bulk interactions, expressed by the change in surface $-\left[\chi_s(dx_1/hx_2) - \chi_s(hx_1/dx_2)\right]$ and bulk parameter $\left[\chi(dx_1/hx_2) - \chi(hx_1/dx_2)\right]$. Each blend pair is marked in Figure 5 by a different symbol. The relations between surface χ_s and bulk χ parameters, presented in Figure 5, are the main finding of this study. Before discussing them we recall in the next section's enthalpic arguments describing bulk and surface interactions. Then we present a possible explanation, also including entropic considerations, followed by remarks on the role of microstructure and isotope labeling.

MISSING-NEIGHBOR EFFECT

Enthalpic Arguments

In the lattice model the bulk interaction parameter χ is expressed⁴³ by the contact energies ε_{ij} between the i and j segments:

$$\chi = \frac{z - 2}{k_B T} [\varepsilon_{AB} - \frac{1}{2}(\varepsilon_{AA} + \varepsilon_{BB})] \quad (7)$$

where z is the coordination number of the lattice. For molecules that are approximately nonpolar, the Van Laar⁴⁴ relation $\varepsilon_{AB} = -(\varepsilon_{AA}\varepsilon_{BB})^{1/2}$ is applicable, and the solubility parameter $\delta_i = [-(z - 2)\varepsilon_{ii}/(2V)]^{1/2}$ may be introduced, related to the cohesive energy density $E_i^{coh} = [-(z - 2)\varepsilon_{ii}/(2V)]$ of the i th polymer. This simplifies the expression for the interaction parameter:

$$\chi = \frac{V}{k_B T} [\delta_A - \delta_B]^2 \quad (8)$$

This formula has been used previously to explain⁶⁻⁸ the label-swapping effect in bulk interactions. The solubility parameter δ is reduced for deuterated molecules and for copolymers with higher EE content x (see inset to Fig. 6). The first change is due to the C—H bond length decreasing

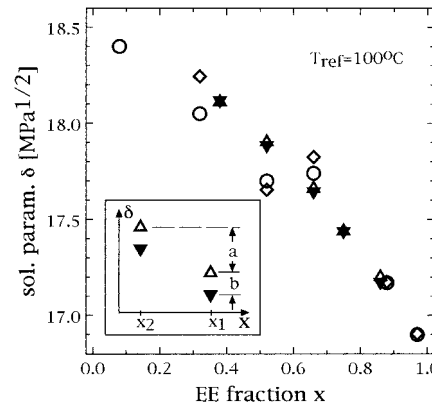


Figure 6. The absolute value of the solubility parameter δ for deuterium labeled (solid triangles) and non-labeled (open triangles) copolymers $E_{1-x}EE_x$ as a function of EE fraction x determined at a reference temperature $T_{ref} = 100^\circ\text{C}$. This relation is based on the phase coexistence data⁹ and the interpolation of the δ values yielded by PVT data^{41,45} at 83°C (◊) and 121°C (○). The inset shows the reduction in δ caused by deuteration ($\Delta\delta = b$) and due to the increase of the EE fraction x ($\Delta\delta = a$).

with deuteration.³ The second variation^{6–8} could be related²⁷ to the monotonic decrease of the statistical segment length^{27,41} with EE fraction x : Higher x copolymers have shorter and thicker segments, which, therefore, have fewer interactions with segments from other chains responsible for the cohesion of the material. Reductions in δ due to isotopic ($\Delta\delta = b$) and microstructural ($\Delta\delta = a$) disparity (see inset to Fig. 6) sum up ($\Delta\delta = a + b$) for the deuterated copolymer with a higher composition x , but reduce $\Delta\delta$ ($\Delta\delta = a - b$) for the blend with swapped-labeled components.

Based on bulk interaction data⁹ and eq. (8), we determine for each blend the solubility parameter difference $\Delta\delta = |\delta_A - \delta_B|$. These results point out the relations between the absolute values of the solubility parameter δ for pure components grouped in two sequences: *h86–d75–h66–d52–h38* and *d86–h75–d66–h52–d38*. Independently, the absolute values of $\delta = 17.2 \text{ MPa}^{1/2}$ for *h86* and $\delta = 17.44 \text{ MPa}^{1/2}$ for *h75*, both at 100°C, were interpolated based on available data on pure component PVT properties.^{41,45} This information allows us to determine, for all polyolefins studied here, the absolute value of the solubility parameter δ plotted in Figure 6 as a function of the EE fraction x for labeled (solid triangles) and nonlabeled (open triangles) copolymers. We find these values in line with the δ values obtained from independent PVT measurements of pure blend components (\diamond, \circ). This shows that the enthalpic arguments alone explain well the miscibility of studied mixtures, a conclusion that has been drawn in earlier studies.^{41,45}

The surface segregation in polymer blends is driven by the net difference χ_s in the surface energy between blend components. An enthalpy-based short-range lattice model describes this net surface difference χ_s^H as given by the following formula¹¹:

$$\chi_s^H = \frac{z_s}{k_B T} [(\varepsilon_{SA} - \varepsilon_{SB}) - \frac{1}{2}(\varepsilon_{AA} - \varepsilon_{BB})] \quad (9)$$

where z_s is the effective number of surface/blend contacts per lattice site.¹¹ The first term in this equation arises from the contact interactions ($\varepsilon_{SA}, \varepsilon_{SB}$) of blend component segments with the surface. The second term accounts for the interactions lost as the surface constrains the blend to a half-space. For the free surface, which is the case studied here, only the second “missing-

neighbor” term $\chi_s^{H,mn}$ is present. It is expressed by the solubility parameters δ_i of both blend components:

$$\chi_s^{H,mn} = \frac{z_s}{z - 2} \frac{V}{k_B T} [\delta_A^2 - \delta_B^2] \quad (10)$$

These enthalpic arguments predict the free-surface segregation of the blend component with lower cohesive energy density (lower δ).

Forces Driving the Segregation

Now we are ready to discuss the relations between surface and bulk interactions presented in Figure 5. Nonzero values of bulk interaction parameter χ read from Figure 5(a) reflect [eq. (8)] distinct differences between solubility parameters of blend components. They result in nonzero and large surface energy difference parameters χ_s expected [eq. (10)] for the missing-neighbor effect. These predictions are not borne out by the experimental results presented in Figure 5(a), where χ_s values close to zero correspond to relatively large bulk interaction parameters χ . We deduce that surface interactions have an additional contribution that reduces their amplitude expected for the pure enthalpic considerations. In turn, a correlation between the label-swapping effect observed for surface and bulk interactions may be concluded based on Figure 5(b). This suggests that the label exchange could modify surface interactions predominantly due to an enthalpic mechanism analogous to that describing bulk interactions.

Following recent theoretical suggestions^{12–16} we propose that the effective surface interaction χ_s parameter is composed of enthalpic $\chi_s^{H,mn}$ and entropic χ_s^S contributions:

$$\chi_s = \chi_s^{H,mn} + \chi_s^S \quad (11)$$

The missing-neighbor component $\chi_s^{H,mn}$ favors the surface segregation of the copolymer with a higher EE fraction x and lower cohesive energy density [Fig. 6 and eq. (1)]. As noted above, this χ_s value is reduced due to the second, entropic term χ_s^S , preferring surface excess in the stiffer blend component with lower EE content x . Recently, Monte Carlo,¹³ MF,²⁴ and self-consistent MF²⁵ studies predict a pronounced¹⁷ surface excess of the stiffer component from the mixtures of stiff and flexible polymer chains. The forces preferring

stiffer polymers at the surface are related by ref. 13(b) to packing entropy and entropy effects due to local rearrangements of segments at the surface.

An essential measure of the polymer stiffness in the models considering entropic segregation is the statistical segment length.^{13b,15,24} The change of the isotopic composition of olefinic copolymers hardly affects their statistical segment lengths,⁴⁶ and only to a small extend the segmental volume ($\Delta V/V \approx 0.2\%$).⁷ Thus, it may be argued that entropical factors driving to surface enrichment would be insensitive, to a first order, to the deuterium labeling of molecules. A similar conclusion has been drawn recently by Donley et al.^{15b} As a result, the entropic contribution χ_s^S is almost identical for a pair of blends x_1/x_2 with a swapped-labeled component, i.e., $\chi_s^S(dx_1/hx_2) \equiv \chi_s^S(hx_1/dx_2)$. Hence, the change in χ_s due to the swap of the deuterated constituent may be related to the missing-neighbor effect alone:

$$\begin{aligned} \chi_s(dx_1/hx_2) - \chi_s(hx_1/dx_2) \\ \equiv \chi_s^{H,mn}(dx_1/hx_2) - \chi_s^{H,mn}(hx_1/dx_2) \end{aligned} \quad (12)$$

Based on eq. (10) and solubility parameters δ of Fig. 6, we calculate the right-hand side of eq. (12) for two values of the ratio $z_s/(z - 2) = 0.5$ and 0.75. Results are marked in Figure 5(b) by a solid and a dashed line, respectively. The ratio $z_s/(z - 2)$, related to the change in the coordination number at the surface, is a constant equal to 0.25 or 0.3 in the lattice models⁴⁷ and an adjustable parameter in experimental studies (e.g., an estimate $0.25 \leq z_s/(z - 2) \leq 0.5$ was obtained for different blends⁴⁸). Figure 5(b) shows that the extent of the label-swapping effect is well explained by enthalpic arguments expressed by eq. (12).⁴⁹

For each blend pair x_1/x_2 the calculations also yield the average value of the enthalpic contribution $\langle \chi_s^{H,mn} \rangle$ shown in Figure 7 for $z_s/(z - 2) = 0.5$ and 0.75. Comparing for each pair x_1/x_2 the average values of the surface parameter $\langle \chi_s \rangle$ and its calculated enthalpic part $\langle \chi_s^{H,mn} \rangle$, we are able to evaluate also the entropic contribution $(-\chi_s^S)$. Both entropic $(-\chi_s^S)$ and enthalpic $\langle \chi_s^{H,mn} \rangle$ components of the surface energy parameter are plotted in Figure 7 as a function of the difference Δn_b in the extent of ethyl branching between copolymers x_1 and x_2 . The magnitude of both contributions seems to depend on chemical mismatch between blend components expressed

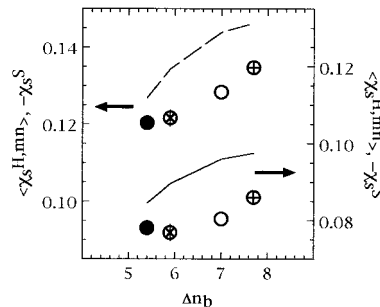


Figure 7. Average enthalpic $\langle \chi_s^{H,mn} \rangle$ (lines) and entropic χ_s^S (symbols) contributions to surface energy difference parameter χ_s plotted as function of the difference Δn_b in the number of ethyl branches between the components x_1 and x_2 of 4 blend pairs x_1/x_2 . These values are for $z_s/(z - 2)$ equal to 0.5 and 0.75 (see lower and higher part of the figure, respectively).

by Δn_b rather than by Δx . Similarly to bulk interactions⁹ the relevant parameter better describing the microstructure is the number of ethyl branches per 100 carbon backbone units $n_b = x/(4 - 2x/100)$ and not the EE fraction x . The magnitude of $(-\chi_s^S)$ is comparable to that of $\langle \chi_s^{H,mn} \rangle$ in accordance with a recent self-consistent MF analysis²⁵: this predicts an equal weight for the missing-neighbor effect and for the entropic mechanism favoring stiffer chains at the surface. The absolute values of $(-\chi_s^S)$ evaluated for $z_s/(z - 2) = 0.5$ are similar to those evaluated previously for entropic segregation (of different origin) in isotopic polystyrene mixtures with chain-length disparity.¹²

The Role of Microstructure and Isotope Labeling

The above analysis reveals a relatively complex relation between surface interactions and microstructural and isotopic characteristics of olefinic copolymers in binary mixtures. The situation in the absence of isotopic effects is illustrated by Figure 7.⁵⁰ Both enthalpic and entropic forces driving the segregation of the copolymer with higher and lower EE content x , respectively, seem to increase with the extent of chemical mismatch Δn_b . However, because they compensate each other, the resulting effective surface interactions do not exhibit a significant dependence on the microstructural difference (Δn_b or Δx) between blend components.

The isotope labeling seems to alter mainly the enthalpic rather than entropic segregation mechanism. The scenario is analogous to that deduced

for bulk interactions (see inset to Fig. 6) coupling the changes in cohesive energy density due to isotopic and microstructural disparity. Surface interactions are predicted to be enhanced/diminished for the deuterated blend component with higher/lower EE fraction x . The missing-neighbor mechanism also accounts for the extent of the label-swapping effect: larger amplitudes are expected for blend components with larger chemical mismatch and larger difference in the fraction of hydrogen replaced by deuterium.⁶

The label-swapping effect results in extended range of surface and bulk interactions centered at their relatively high values. This range is, however, shifted down for the surface parameter χ_s due to additional entropic contribution. As a result, the isostructural blend pairs dx_1/hx_2 and hx_1/dx_2 have a large disparity in the absolute values of surface χ_s but not in the bulk χ parameter [see Fig. 5(a)]. This leads to completely different types of surface phase diagrams. For instance, the $d66/h52$ mixture exhibits²⁸ an extended critical wetting region ($T_c - T_w > 100$ deg), while its swapped counterpart $h66/d52$ shows²⁹ behavior typical for a wetting point T_w located close to T_c ($T_c - T_w < 10$ deg).

Most of theoretical models applicable to the mixtures of random olefinic copolymers $E_{1-x}EE_x$ treat them as linear chains with effective properties, such as segment length or cohesive energy, tuned by EE fraction x . However, additional mechanisms driving segregation are plausible for copolymers with an ordered sequence of building blocks E and EE. Consider, for instance, the effects due to local rearrangements of segments in the immediate vicinity of a surface.^{13b} When a chain segment is located exactly at the surface, then the probability that the next segment of the same chain will also be at the surface is larger for a stiff chain than it is for a flexible chain. This effect would be much stronger in the case of blocks with stiff segments. The effect of segment sequencing also influences the cohesive energy density (compare, e.g., data for the mixtures of $d78$ with random $h66$ and alternating $hPEB$ ^{41a}) and, hence, it would also change the enthalpic forces driving the segregation.

SUMMARY AND CONCLUSIONS

We have performed a cumulative analysis of the segregation observed at a wide temperature range at the free surface of eight blends formed by

random olefinic copolymers $E_{1-x}EE_x$. We determined a surface-energy difference parameter χ_s and found out that its value changes when the blend component labeled by deuterium is swapped. The pattern and the magnitude of this change for a surface parameter χ_s is related to that for the bulk interaction parameter χ , reported earlier.⁶⁻⁹ Although bulk interactions are well explained by enthalpic arguments alone^{41,45} the comparison of surface χ_s and bulk χ parameters reveals that surface interactions have also an important entropic contribution, in accordance with theoretical expectations.^{12-16,25} Copolymers with higher ethyl ethylene (EE) content x and lower cohesive energy density are attracted to the free surface by enthalpic forces. The stiffer chains with a lower EE fraction x are driven there by an entropy-related mechanism. This causes the observed surface excess to be reduced compared with purely enthalpic predictions. The change in χ_s upon isotope label swapping is accounted for by enthalpic effects, while entropic forces are argued^{15b} to be hardly sensitive to the isotopic status of the polymers. It is found that the strength of both segregation mechanisms seems to depend on the extent of chemical mismatch, expressed by the difference Δn_b in extent of ethyl branching between the blend components. The effect of entropy on surface segregation observed here for short-branched polymers is comparable to the enthalpic contributions. It does not dominate over the enthalpic effects, as was observed recently for long-branched chain additives in the linear polymer matrix,^{17,21} or for the mixtures of linear polymers with chain-length disparity.¹²

Useful discussions with Drs. Sanat Kumar and Gregory T. Dee are acknowledged with appreciation. We also thank for a partial financial support for these studies provided by the Reserve for Individual Research of the Rector of Jagellonian University, the Minerva Foundation, the Israeli Science Foundation, and the Ministry of Sciences and Arts (Israel) (Tashtit program).

REFERENCES AND NOTES

1. K. Binder, *Acta Polym.*, **46**, 204 (1995).
2. (a) I. C. Sanchez, *Annu. Rev. Mater. Sci.*, **13**, 387 (1983); (b) R. Koningsveld, L. A. Kleintjens and E. Nies, *Croatica Chem. Acta*, **60**, 53 (1987); (c) F. S. Bates, *Science*, **251**, 898 (1991).
3. F. S. Bates, G. D. Wignall, and W. C. Kohler, *Phys. Rev. Lett.*, **55**, 2425 (1985).

4. (a) A. Budkowski, U. Steiner, J. Klein, and G. Schatz, *Europhys. Lett.*, **18**, 705 (1992); (b) J. D. Londono, A. H. Narten, G. D. Wignall, K. G. Honel, E. T. Hiseh, T. W. Johnson, and F. S. Bates, *Macromolecules*, **27**, 2864 (1994).
5. J. Rhee and B. Crist, *Macromolecules*, **24**, 5663 (1991).
6. A. Budkowski, J. Klein, E. Eiser, U. Steiner, and L. J. Fetter, *Macromolecules*, **26**, 3858 (1993).
7. J. Rhee and B. Crist, *J. Chem. Phys.*, **98**, 4174 (1993).
8. W. W. Graessley, R. Krishnamoorti, N. P. Balsara, L. J. Fetter, D. J. Lohse, D. N. Schulz, and J. A. Sissano, *Macromolecules*, **26**, 1143 (1993).
9. F. Scheffold, E. Eiser, A. Budkowski, U. Steiner, J. Klein, and L. J. Fetter, *J. Chem. Phys.*, **104**, 8786 (1996).
10. (a) R. A. J. Jones, E. J. Kramer, M. H. Rafailovich, J. Sokolov, and S. Schwartz, *Phys. Rev. Lett.*, **62**, 280 (1989); (b) A. Budkowski, U. Steiner, and J. Klein, *J. Chem. Phys.*, **97**, 5229 (1992); (c) L. J. Norton, E. J. Kramer, F. S. Bates, M. D. Gehlsen, R. A. L. Jones, A. Karim, G. P. Felcher, and R. Kleb, *Macromolecules*, **28**, 8621 (1995).
11. (a) A. Hariharan, S. K. Kumar, and T. P. Russell, *Macromolecules*, **24**, 4909 (1991); (b) R. A. Jerry and E. B. Nauman, *Phys. Lett. A*, **167**, 198 (1992).
12. A. Hariharan, S. K. Kumar, and T. P. Russell, *J. Chem. Phys.*, **98**, 4163 (1993).
13. (a) A. Yethiraj, S. Kumar, A. Hariharan, and K. S. Schweizer, *J. Chem. Phys.*, **100**, 4691 (1994); (b) S. Kumar, A. Yethiraj, K. S. Schweizer, and F. A. M. Leermakers, *J. Chem. Phys.*, **103**, 10332 (1995).
14. A. Yethiraj, *Phys. Rev. Lett.*, **74**, 2018 (1995).
15. (a) D. T. Wu, G. H. Fredrickson, and J.-P. Carton, *J. Chem. Phys.*, **104**, 6387 (1996); (b) J. P. Donley, D. T. Wu, and G. H. Fredrickson, *Macromolecules*, **30**, 2167 (1997).
16. D. T. Wu and G. H. Fredrickson, *Macromolecules*, **29**, 7919 (1996).
17. A. Mayes and S. K. Kumar, *MRS Bull.*, **January**, 43 (1997).
18. A. Hariharan, S. K. Kumar, and T. P. Russell, *Macromolecules*, **23**, 3584 (1990).
19. S. Cohen and M. Muthukumar, *J. Chem. Phys.*, **90**, 5749 (1989).
20. D. G. Walton and A. M. Mayes, *Phys. Rev. E*, **54**, 2811 (1996).
21. D. G. Walton, P. P. Soo, A. M. Mayes, S. J. Sofia Allgor, J. T. Fujii, L. G. Griffith, J. F. Anker, H. Keiser, J. Johansson, G. D. Smith, J. G. Baker, and S. K. Satija, *Macromolecules*, **30**, 6947 (1997).
22. G. H. Fredrickson and J. P. Donley, *J. Chem. Phys.*, **97**, 8941 (1992).
23. M. Sikka, N. Singh, A. Karim, F. S. Bates, S. K. Satija, and C. F. Majkrzak, *Phys. Rev. Lett.*, **70**, 307 (1993).
24. M. A. Carigano and I. Szleifer, *Europhys. Lett.*, **30**, 525 (1995).
25. C. C. van der Linden, F. A. M. Leermakers, and G. J. Fleer, *Macromolecules*, **29**, 1172 (1996).
26. (a) U. Steiner, J. Klein, E. Eiser, A. Budkowski, and J. F. Fetter, *Science*, **258**, 1126 (1992); (b) U. Steiner, J. Klein, and L. J. Fetter, *Phys. Rev. Lett.*, **72**, 1498 (1994); (c) U. Steiner, E. Eiser, A. Budkowski, L. J. Fetter, and J. Klein, *Ber. Bunsenges. Phys. Chem.*, **98**, 366 (1994); (d) U. Steiner and J. Klein, *Phys. Rev. Lett.*, **77**, 2526 (1996).
27. F. Scheffold, A. Budkowski, U. Steiner, E. Eiser, J. Klein, and L. J. Fetter, *J. Chem. Phys.*, **104**, 8795 (1996).
28. A. Budkowski, F. Scheffold, J. Klein, and L. J. Fetter, *J. Chem. Phys.*, **106**, 719 (1997).
29. A. Budkowski, J. Rysz, F. Scheffold, J. Klein, *Europhys. Lett.*, in press.
30. U. K. Chaturvedi, U. Steiner, O. Zak, G. Krausch, G. Schatz, and J. Klein, *Appl. Phys. Lett.*, **56**, 1228 (1990).
31. J. W. Cahn, *J. Chem. Phys.*, **66**, 3667 (1977).
32. P.-G. de Gennes, *J. Chem. Phys.*, **72**, 4756 (1980).
33. I. Schmidt and K. Binder, *J. Physique*, **46**, 1631 (1985).
34. R. A. Jerry and A. Dutta, *J. Colloid Interface Sci.*, **167**, 287 (1994).
35. S. K. Kumar, H. Tang, and I. Szleifer, *Mol. Phys.*, **4**, 867 (1994).
36. F. Bruder and R. Brenn, *Europhys. Lett.*, **22**, 707 (1993).
37. R. A. L. Jones and E. J. Kramer, *Polymer*, **34**, 115 (1993).
38. S. K. Kumar and T. P. Russell, *Macromolecules*, **24**, 3816 (1991).
39. J. Genzer, A. Falda, R. Oslanec, and R. J. Composto, *Macromolecules*, **29**, 5438 (1996).
40. B. Guckenbühl, M. Stamm, and T. Springer, *Colloid Surface A: Physicochem. Eng. Aspects*, **86**, 311 (1994).
41. (a) R. K. Krishnamoorti, W. W. Graessley, N. P. Balsara, and D. J. Lohse, *Macromolecules*, **27**, 3073 (1994); (b) W. W. Graessley, R. Krishnamoorti, G. C. Reichart, N. P. Balsara, L. J. Fetter, and D. J. Lohse, *Macromolecules*, **28**, 1260 (1995).
42. (a) J. W. Cahn and J. E. Hilliard, *J. Chem. Phys.*, **28**, 258 (1958); (b) S. Wu, *Polymer Interface and Adhesion*, Marcel Dekker, New York, 1982.
43. (a) P. J. Flory, *Principles of Polymer Chemistry*, Cornell Univ., Ithaca, NY, 1975; (b) P.-G. de Gennes, *Scaling Concepts in Polymer Physics*, Cornell Univ., Ithaca, NY, 1979.
44. J. J. van Laar and R. Lorenz, *Z. Anorg. Allgem. Chem.*, **146**, 42 (1925).
45. W. W. Graessley, R. Krishnamoorti, N. P. Balsara, R. J. Butera, L. J. Fetter, D. J. Lohse, D. N. Schulz, and J. A. Sissano, *Macromolecules*, **27**, 3896 (1994).

46. N. P. Balsara, L. J. Fetters, N. Hadjichristidis, D. J. Lohse, C. C. Han, W. W. Graessley, and R. Krishnamoorti, *Macromolecules*, **25**, 6137 (1992); N. P. Balsara, D. J. Lohse, W. W. Graessley, and R. Krishnamoorti, *J. Chem. Phys.*, **100**, 3905 (1994).
47. H. Tang, I. Szleifer, and S. K. Kumar, *J. Chem. Phys.*, **100**, 5367 (1994).
48. S. Reich and Y. Cohen, *J. Polym. Sci., Polym. Phys. Ed.*, **19**, 1255 (1981).
49. The misfit observed for the 66/52 blend pair might be related to a smaller enthalpic contribution to the bulk interaction parameter χ (evaluated as 80% for this blend pair, but higher than 94% for the other blends,⁹ and assumed as 100% in the evaluations of the missing neighbor effect).
50. This is because $(-\chi_s^S)$ is hardly sensitive to deuteration while $\langle\chi_s^{H,mn}\rangle$ is equivalent to the average value for blends dx_1/dx_2 and hx_1/hx_2 .